



Synthesis and photoinduced surface relief grating formation of novel photo-responsive amorphous molecular materials, 4-[bis(9,9-dimethylfluoren-2-yl)amino]-4'-cyanoazobenzene and 4-[bis(9,9-dimethylfluoren-2-yl)-amino]-4'-nitroazobenzene

Hideyuki Nakano^{a,*}, Toru Takahashi^a, Takahiro Tanino^a, Yasuhiko Shirota^{a,b}

^a Department of Applied Chemistry, Faculty of Engineering, Osaka University, Yamadaoka, Suita, Osaka 565-0871, Japan

^b Department of Environmental and Biotechnological Frontier Engineering, Fukui University of Technology, 3-6-1, Gakuen, Fukui City, Fukui 910-8505, Japan

ARTICLE INFO

Article history:

Received 18 April 2009

Received in revised form

1 July 2009

Accepted 1 July 2009

Available online 8 July 2009

Keywords:

Photo-responsive amorphous molecular material

Photoinduced surface relief grating formation

Azobenzene

trans–cis Photoisomerization

Glass-transition temperature

ABSTRACT

Novel azobenzene-based photo-responsive amorphous molecular materials, 4-[bis(9,9-dimethylfluoren-2-yl)amino]-4'-cyanoazobenzene and 4-[bis(9,9-dimethylfluoren-2-yl)amino]-4'-nitroazobenzene, have been synthesized and the formation of surface relief grating on their amorphous films has been investigated. It was found that a relatively large surface relief grating could be inscribed on both amorphous films upon interference exposure to the writing laser beams. The modulation depth of the surface relief grating inscribed on the amorphous film of the cyano-substituted material was found to be larger than that inscribed on the film of the nitro-substituted one and seemed to be comparable to that inscribed on the amorphous film of the parent material, 4-[bis(9,9-dimethylfluoren-2-yl)amino]azobenzene. These results were discussed from the viewpoint of their trans–cis photoisomerizations as amorphous films and glass-transition temperatures.

© 2009 Elsevier Ltd. All rights reserved.

1. Introduction

Recently, mechanical motions of materials induced by photo-irradiation, so-called “photomechanical effects”, have attracted a great deal of attention. Several examples of the photomechanical effects observed for photochromic materials, such as bending of liquid–crystalline azo-polymer network films [1] and reversible shape changes of molecular crystals of diarylethene derivatives [2], have been reported. Photoinduced surface relief grating (SRG) formation observed for films of azobenzene-based materials, which is induced by mass transport upon interference exposure to coherent laser beams, is also an attractive subject as one of the photomechanical effects. A number of studies of photoinduced SRG formation have been made using a variety of systems including azobenzene-based amorphous polymers [3–11], azobenzene-based liquid–crystalline films [12–17], poly(methyl methacrylate) films doped with spiropyran [18] and diarylethene derivatives [19], and

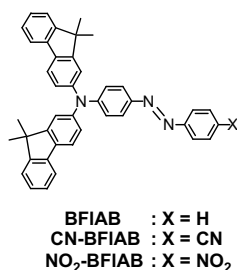
photocrosslinkable polymer liquid crystals [20,21]. With regard to photoinduced SRG formation using azobenzene-based materials, it is believed that the mass transport is induced by trans–cis and cis–trans isomerizations of the azobenzene chromophore to produce the SRG. Several models for the mechanism of the photoinduced SRG formation have been proposed [5–9,17,22]; however, the precise details are not yet clear.

In contrast to the foregoing polymeric systems, we have studied the photoinduced SRG formation using azobenzene-based photo-responsive amorphous molecular materials, namely, low molecular-weight photo-responsive molecules that form amorphous glasses by themselves [23–27]. In addition, we have demonstrated very recently that photoinduced SRG formation can take place even on the single crystals of azobenzene-based materials [28–30]. With regard to photo-responsive amorphous molecular materials, relatively large SRG with a modulation depth of more than 400 nm could be inscribed on an amorphous film of 4-[bis(9,9-dimethylfluoren-2-yl)amino]azobenzene (BFIAB) [27]. In addition, the increase of glass-transition temperature (T_g) of the material was found to be favorable for photoinduced SRG formation [27]. Photoinduced SRG formation using amorphous molecular materials

* Corresponding author. Tel.: +81 6 6879 7365; fax: +81 6 6879 7367.

E-mail address: nakano@chem.eng.osaka-u.ac.jp (H. Nakano).

has also been reported by other groups [31–35]. However, the phenomena using photo-responsive amorphous molecular materials remain to be fully elucidated and therefore it is of importance to elucidate SRG-forming properties of a variety of azobenzene-based photo-responsive amorphous molecular materials in relation to their molecular structures, Tgs, reactivity, and other properties. In the present study, we have designed and synthesized novel azobenzene-based photo-responsive amorphous molecular materials possessing either a cyano- or a nitro-substituent at the 4'-position of the azobenzene moiety of BFIAB, i.e. 4-[bis(9,9-dimethylfluoren-2-yl)amino]-4'-cyanoazobenzene (CN-BFIAB) and 4-[bis(9,9-dimethylfluoren-2-yl)amino]-4'-nitroazobenzene (NO₂-BFIAB) [36], and investigated photoinduced SRG formation on their amorphous films.



2. Experimental

2.1. Materials

4-Nitroaniline, 4-cyanoaniline, and 4-amino-4'-nitroazobenzene were purchased (Tokyo Chemical Industry Co., Ltd.) and used without further purification. 2-Iodo-9,9-dimethylfluorene was synthesized according to the previously described procedure [37].

2.2. *N,N'*-Bis(9,9-dimethylfluoren-2-yl)-4-nitroaniline (**1**)

2-Iodo-9,9-dimethylfluorene (136 g, 430 mmol) and 4-nitroaniline (24.1 g, 170 mmol) were heated under reflux in the presence of copper powder (27.0 g, 430 mmol), K₂CO₃ (110.5 g, 800 mmol) and 18-crown-6 (8.5 g, 50 mmol) in mesitylene (300 ml) for 8 h under nitrogen atmosphere. After the solvent was removed under reduced pressure, the residue was extracted with toluene and washed with water. The product was purified by silica-gel column chromatography using a mixed solvent of toluene and hexane as an eluent. Yield: 56.3 g (63%), m.p.: 147 °C. MS: *m/z* 522 (M⁺). ¹H NMR (750 MHz, THF): δ 8.06 (dd, 2.1, 7.2 Hz, 2H), 7.76 (d, 8.0 Hz, 2H), 7.72 (d, 7.4 Hz, 2H), 7.44 (d, 7.4 Hz, 2H), 7.39 (d, 2.0 Hz, 2H), 7.30 (ddd, 1.1, 7.4, 7.4 Hz, 2H), 7.26 (ddd, 1.1, 7.4, 7.4 Hz, 2H), 7.19 (dd, 2.0, 8.0 Hz, 2H), 7.10 (dd, 2.1, 7.2 Hz, 2H), 1.42 (s, 12H) ppm. ¹³C NMR (188 MHz, THF): δ 156.5, 154.7, 154.6, 146.4, 141.5, 139.4, 137.7, 128.0, 127.9, 126.0, 126.0, 123.4, 122.0, 121.5, 120.6, 119.9, 47.7, 27.2 ppm.

2.3. 4-[Bis(9,9-dimethylfluoren-2-yl)amino]-4'-cyanoazobenzene (CN-BFIAB)

4-Aminobenzonitrile (0.47 g, 4 mmol) and **1** (1.56 g, 3 mmol) were heated under reflux in the presence of NaOH (0.85 g, 21 mmol) in mesitylene (10 ml) for 1 h under nitrogen atmosphere. After the solvent was removed under reduced pressure, the residue was extracted with toluene and washed with water. The product was purified by silica-gel column chromatography using a mixed solvent of toluene and hexane as an eluent, followed by recrystallization from cyclohexane. Yield: 600 mg (33%), m.p.: 236 °C. MS:

m/z 606 (M⁺). ¹H NMR (750 MHz, THF): δ 7.96 (d, 8.3 Hz, 2H), 7.87 (d, 8.8 Hz, 2H), 7.86 (d, 8.3 Hz, 2H), 7.73 (d, 8.1 Hz, 2H), 7.71 (d, 7.4 Hz, 2H), 7.43 (d, 7.4 Hz, 2H), 7.38 (s, 2H), 7.29 (dd, 7.4, 7.4 Hz, 2H), 7.25 (dd, 7.4, 7.4 Hz, 2H), 7.22 (d, 8.8 Hz, 2H), 7.19 (dd, 8.1 Hz, 2H), 1.42 (s, 12H) ppm. ¹³C NMR (188 MHz, THF): δ 156.4, 155.9, 154.6, 153.0, 147.8, 147.1, 139.6, 137.0, 134.1, 127.9, 127.8, 125.8, 125.6, 123.8, 123.3, 122.0, 121.8, 121.0, 120.5, 118.9, 114.3, 47.7, 27.2 ppm. EA: Calcd for C₄₃H₃₄N₄: C, 85.12; H, 5.65; N, 9.23%. Found: C, 84.98; H, 5.82; N, 9.01%.

2.4. 4-[Bis(9,9-dimethylfluoren-2-yl)amino]-4'-nitroazobenzene (NO₂-BFIAB)

4-Amino-4'-nitroazobenzene (3.7 g, 0.015 mol) and 2-iodo-9,9-dimethylfluorene (12 g, 0.037 mol) were heated under reflux in the presence of copper powder (2.4 g, 0.037 mol), K₂CO₃ (6.5 g, 0.047 mol) and 18-crown-6 (0.7 g, 0.026 mol) in mesitylene (50 ml) for 4 h under nitrogen atmosphere. After the solvent was removed under reduced pressure, the residue was extracted with toluene and washed with water. The product was purified by silica-gel column chromatography using a mixed solvent of toluene and hexane as an eluent, followed by recrystallization from cyclohexane. Yield: 3.5 g (37%), m.p.: 228 °C. MS: *m/z* 626 (M⁺). ¹H NMR (750 MHz, THF): δ 8.37 (d, 9.0 Hz, 2H), 8.01 (d, 9.0 Hz, 2H), 7.89 (d, 8.9 Hz, 2H), 7.74 (d, 8.1 Hz, 2H), 7.72 (d, 7.4 Hz, 2H), 7.43 (d, 7.4 Hz, 2H), 7.39 (d, 1.9 Hz, 2H), 7.29 (dd, 7.4, 7.5 Hz, 2H), 7.26 (dd, 7.4, 7.5 Hz, 2H), 7.23 (d, 8.9 Hz, 2H), 7.20 (dd, 1.9, 8.1 Hz, 2H), 1.43 (s, 12H) ppm. ¹³C NMR (188 MHz, THF): δ = 157.2, 156.4, 154.6, 153.2, 149.3, 147.9, 147.0, 139.6, 137.1, 127.9, 127.8, 126.0, 125.6, 125.5, 123.7, 123.3, 121.9, 121.8, 121.1, 120.5, 47.4, 27.2 ppm. EA: Calcd for C₄₂H₃₄N₄O₂: C, 80.49; H, 5.47; N, 8.94%. Found: C, 80.31; H, 5.58; N, 8.71%.

2.5. Measurements and apparatus

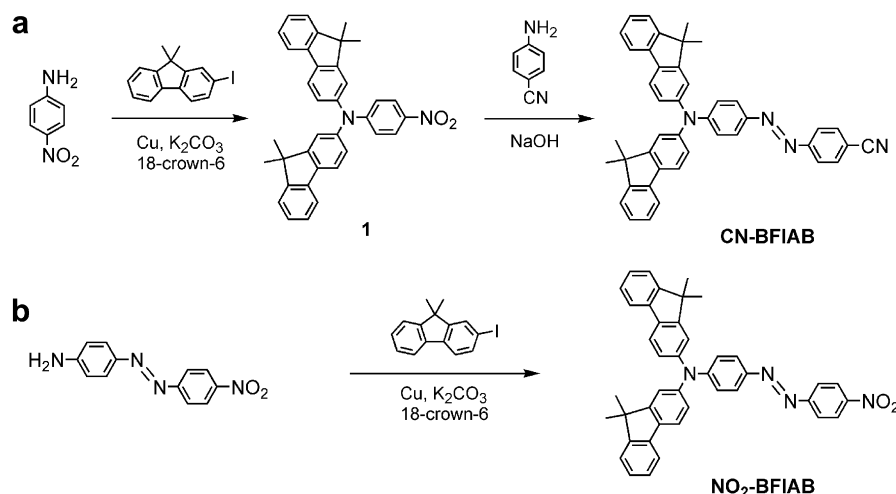
Differential scanning calorimetry (DSC) was carried out by means of a Seiko DSC220C. Photoisomerization was carried out by irradiation of the amorphous films with 500 nm light with a bandwidth of 10 nm from a 500 W Xenon lamp (UXL-500D, USHIO) through an interference filter (IF-S 500, Vacuum Optics Co.) using an optical fiber. The reactions were monitored by the change in the electronic absorption spectra by means of a Hitachi U-3200 spectrophotometer.

Photoinduced SRG formation was carried out by using an Ar⁺ laser (488 nm: BeamLok 2060, Spectra Physics) as writing beams and a semiconductor laser (830 nm: LDP-8340, NEOARK) as a probe beam at ambient temperature (ca. 30 °C). Sample thickness of CN-BFIAB and NO₂-BFIAB films for SRG formation was ca. 200 μm. Atomic force microscopy (AFM) was performed by means of JSTM-4200D (JEOL) with a micro cantilever (OMCL-AC160 T-C2, OLYMPUS).

3. Results and discussion

3.1. Synthesis and glass-forming properties of CN-BFIAB and NO₂-BFIAB

A novel photo-responsive amorphous molecular material, CN-BFIAB, was synthesized by the condensation reaction of *N,N'*-bis(9,9-dimethylfluoren-2-yl)-4-nitroaniline (**1**) and 4-aminobenzonitrile (Scheme 1a). The Ullmann reaction between 4-amino-4'-nitroazobenzene and 2-iodo-9,9-dimethylfluorene afforded another novel photo-responsive amorphous molecular material, NO₂-BFIAB (Scheme 1b). Both new compounds were identified by various spectroscopy, mass spectrometry, and elemental analysis.



Scheme 1. Synthesis of a) CN-BFIAB and b) NO₂-BFIAB.

Both CN-BFIAB and NO₂-BFIAB were found to readily form amorphous glasses by cooling their molten samples on standing in air. Fig. 1 shows DSC curves of CN-BFIAB and NO₂-BFIAB. When crystalline samples of CN-BFIAB and NO₂-BFIAB obtained by recrystallization from solution were heated, endothermic peaks due to melting were observed at 236 °C and 228 °C, respectively. When the molten samples were cooled on standing in air, amorphous glasses were readily obtained. When the glasses were again heated, baseline shifts due to a glass-transition were observed at 116 °C and 117 °C, respectively, being higher than the T_g of the parent material, BFIAB (97 °C). On further heating, no crystallization phenomena were observed, suggesting that the amorphous glasses were fairly stable [38].

3.2. Photo and thermal isomerizations of CN-BFIAB and NO₂-BFIAB

Both CN-BFIAB and NO₂-BFIAB were found to exhibit trans–cis photoisomerizations and reverse cis–trans thermal isomerizations as amorphous films as well as in solution. Fig. 2 shows electronic absorption spectral changes of CN-BFIAB and NO₂-BFIAB as amorphous films. When the films were irradiated with 500 nm light, the absorbance around 510 nm gradually decreased due to trans–cis photoisomerization. When the irradiation was stopped after the reaction system reached to photostationary state, the absorbance

gradually increased due to the reverse cis–trans thermal isomerization.

The fraction of the photogenerated cis-isomer at the photostationary state (Y_{pss}) can be estimated experimentally from the following equation;

$$Y_{\text{pss}} = \left[1 - \left(A_{\text{pss}}^{\lambda} / A_{\text{trans}}^{\lambda} \right) \right] / \left[1 - \left(\varepsilon_{\text{cis}}^{\lambda} / \varepsilon_{\text{trans}}^{\lambda} \right) \right] \quad (1)$$

where $\varepsilon_{\text{trans}}^{\lambda}$ and $\varepsilon_{\text{cis}}^{\lambda}$ represent the molar extinction coefficients of the trans- and cis-isomers at a measured wavelength λ , $A_{\text{trans}}^{\lambda}$ and A_{pss}^{λ} the absorbance of the sample at the same wavelength before photoirradiation and at the photostationary state, respectively. Since the cis-isomers could not be isolated because of their instability in solution, the value of $\varepsilon_{\text{cis}}^{\lambda}$ was estimated by the spectral changes of the solution upon irradiation with two different wavelengths (400 nm and 450 nm) as described in our previous paper [39]. Table 1 summarizes optical and reaction parameters including wavelength of absorption maximum before photoirradiation (λ_{max}), molar extinction coefficients of trans- and cis-form at λ_{max} ($\varepsilon_{\text{trans}}^{\lambda_{\text{max}}}$ and $\varepsilon_{\text{cis}}^{\lambda_{\text{max}}}$, respectively), cis-fraction at photostationary state (Y_{pss}) upon irradiation with 500 nm light, and first-order rate constant of reverse cis–trans thermal isomerization at 30 °C (k) in toluene solution and as amorphous films for CN-BFIAB and NO₂-BFIAB. The values for BFIAB are also indicated in Table 1 for comparison.

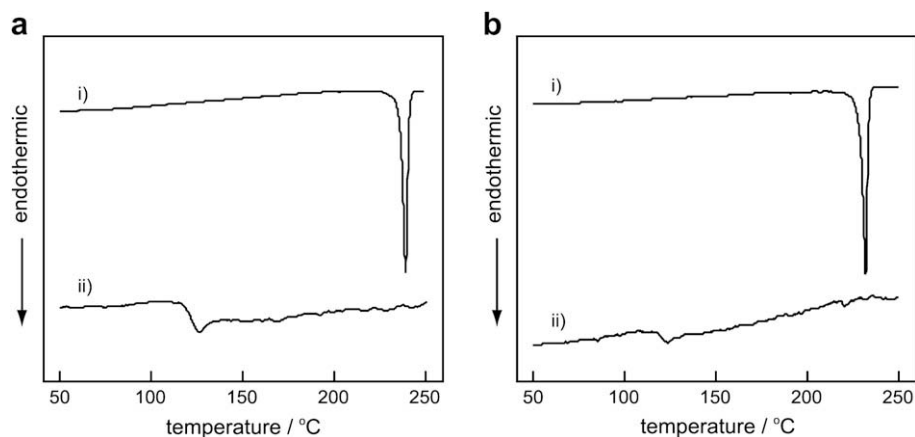


Fig. 1. DSC curves of a) CN-BFIAB and b) NO₂-BFIAB. i) Crystalline sample obtained by recrystallization from solution. ii) Amorphous glass obtained by cooling the molten sample. Heating rate: 5 °C min^{−1}.

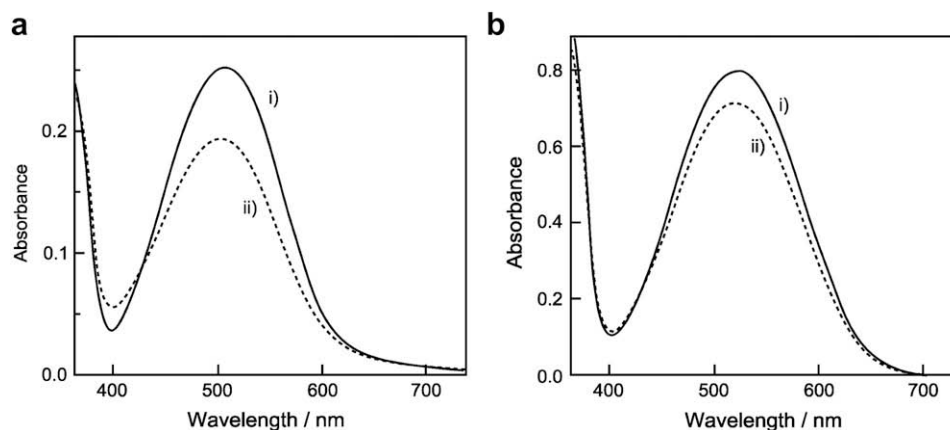


Fig. 2. Electronic absorption spectral changes of a) CN-BFIAB and b) NO₂-BFIAB amorphous films. i) Before photoirradiation. ii) Photostationary state upon irradiation with 500 nm light.

Both λ_{\max} values in solution and as amorphous films for CN-BFIAB and NO₂-BFIAB were found to be red-shifted relative to those for BFIAB. The result was due to the effect of introduction of electron-withdrawing cyano- and nitro-groups into the 4'-position of the azobenzene moiety in the parent BFIAB. The λ_{\max} values as amorphous films for CN-BFIAB and NO₂-BFIAB were slightly red-shifted from those in toluene solution as well as that for the parent BFIAB due to intermolecular interaction. The magnitude of the λ_{\max} shifts for CN-BFIAB and NO₂-BFIAB was not too different from that for BFIAB, suggesting that the degree of the intermolecular interaction as amorphous films for CN-BFIAB and NO₂-BFIAB was not so much different from that for BFIAB.

It was found that the Y_{pss} values for all the present materials were smaller for the amorphous films than in solutions, similar to the result observed for other azobenzene-based photo-responsive amorphous molecular materials we have previously reported [39]. The reactions as amorphous films were suggested to be suppressed relative to that in solution due to small local free volume as amorphous films. The ratio of Y_{pss} for amorphous film to that for toluene solution (R), which was assumed to give an indication of the extent of suppression of the photoisomerizations as amorphous films relative to those in solution, was also summarized in Table 1. It was found that the R value decreased in the order, BFIAB > CN-BFIAB > NO₂-BFIAB, suggesting that the extent of the suppression of the reaction increased in the order, BFIAB < CN-BFIAB < NO₂-BFIAB. It is conceivable that the volume required to facilitate the isomerization becomes larger in this order and hence the reaction in the small local free volume in the amorphous film was suppressed to a greater extent, i.e. quantum yield of trans-cis photoisomerization was reduced, for the material with more bulky substituent at the 4'-position of azobenzene moiety.

Like a variety of azobenzene derivatives, the reverse cis-trans thermal isomerization reactions of CN-BFIAB and NO₂-BFIAB in toluene solution followed the first-order kinetics with the first-order rate constants (k) of 2.2×10^{-2} and $1.1 \times 10^{-1} \text{ min}^{-1}$ at 30 °C, respectively (Table 1). On the other hand, the cis-trans thermal isomerization reactions of CN-BFIAB and NO₂-BFIAB as amorphous films after the reaction system has reached the photostationary state by irradiation with 500 nm light did not follow the expected first-order kinetics and their apparent rate constant at initial stage (k') was larger than those in solution. This phenomenon was similar to that observed for BFIAB [39] and suggested that there exists cis-isomers trapped in constrained conformations in the amorphous film which go back faster into the trans-isomer than the structurally relaxed cis-isomer molecules.

3.3. Photoinduced SRG formation of CN-BFIAB and NO₂-BFIAB

Using the novel photo-responsive amorphous molecular materials, CN-BFIAB and NO₂-BFIAB, photoinduced SRG formation has been investigated. The schematic experimental setup was illustrated in Fig. 3. The amorphous film with a thickness of ca. 200 μm was irradiated with two writing beams (Ar⁺ laser: 488 nm) with polarization angles of +45° and -45° with respect to the p-polarization at 10 mW (ca. 80 mWcm⁻²) each. SRG formation was monitored by diffraction efficiency, which was defined here as the intensity ratio of the first diffraction beam to the incident beam of the probe (laser diode: 830 nm).

As Fig. 4 shows, the diffraction efficiencies gradually increased with exposure time and were finally saturated at ca. 19% and 14% for CN-BFIAB and NO₂-BFIAB, respectively. SRG formation was confirmed by AFM. For CN-BFIAB, SRG with a modulation depth of

Table 1
Optical and reaction parameters in toluene solution and as amorphous film.

Material	Toluene solution					Amorphous film			R^d
	λ_{\max} (nm)	$\epsilon_{\text{trans}}^{\lambda_{\max}}$ (M ⁻¹ cm ⁻¹)	$\epsilon_{\text{cis}}^{\lambda_{\max}}$ (M ⁻¹ cm ⁻¹)	Y_{pss}^a	k (min ⁻¹) ^b	λ_{\max} (nm)	Y_{pss}^a	k' (min ⁻¹) ^c	
CN-BFIAB	494	3.1×10^4	8.0×10^3	0.67 ^e	2.2×10^{-2}	508	0.33 ^e	1.4×10^{-1}	0.49
NO ₂ -BFIAB	513	3.0×10^4	7.9×10^3	0.54 ^e	1.1×10^{-1}	522	0.14 ^e	2.8×10^{-1}	0.26
BFIAB ^g	451	2.7×10^4	7.0×10^3	0.74 ^f	4.7×10^{-3}	461	0.48 ^f	1.5×10^{-2}	0.65

^a Y_{pss} : cis-fraction at photostationary state.

^b k : first-order rate constant of cis-trans thermal isomerization at 30 °C.

^c k' : apparent first-order rate constant of cis-trans thermal isomerization at 30 °C at initial stage (10 s).

^d $R = [Y_{\text{pss}} \text{ as amorphous film}] / [Y_{\text{pss}} \text{ in toluene solution}]$.

^e Upon irradiation with 500 nm light.

^f Upon irradiation with 450 nm light.

^g Reference [39].

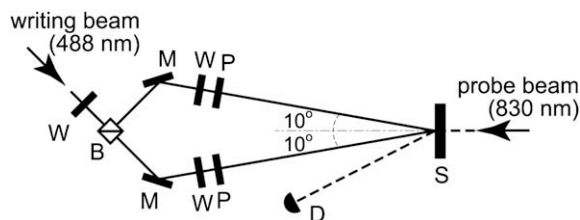


Fig. 3. Experimental setup of photoinduced SRG formation.

400–430 nm was clearly observed as shown in Fig. 5. SRG with a modulation depth of 310–350 nm was also observed for NO₂-BFIAB by AFM. Thus, relatively large SRG could be inscribed on the amorphous films of CN-BFIAB and NO₂-BFIAB.

The modulation depth of SRG inscribed on the CN-BFIAB amorphous film was larger than that inscribed on the NO₂-BFIAB film. As discussed in our previous paper [27], it is thought that photoinduced SRG formation using photo-responsive amorphous molecular materials is influenced by both the photoinduced reaction as amorphous film and T_g of the material, that is, the increasing frequency of trans–cis and cis–trans isomerization cycles facilitates the mass transport to grow SRG and increasing T_g of the material prevents the collapse of the SRG due to surface tension to make the surface smooth. Since T_g of NO₂-BFIAB was almost the same as that of CN-BFIAB, the smaller modulation depth for NO₂-BFIAB than that for CN-BFIAB was suggested to be mainly due to the fact that the quantum yield of trans–cis photoisomerization was lower for NO₂-BFIAB than for CN-BFIAB as described above. Thus, introduction of bulky substituent at 4'-position of azobenzene moiety in BFIAB makes unfavorable for photoinduced SRG formation.

However, the modulation depth of SRG inscribed on CN-BFIAB amorphous film seemed to be comparable to that inscribed on the amorphous film of BFIAB under the similar conditions (450–490 nm) [27] even though the photoisomerization was more suppressed as amorphous film than that for BFIAB. The result indicated that the SRG-forming property of CN-BFIAB was not significantly reduced by introduction of the cyano-substituent into BFIAB. It is conceivable that the higher T_g of CN-BFIAB resulted in the effective enhancement of SRG-forming property, compensating the effect of the suppression of the reaction.

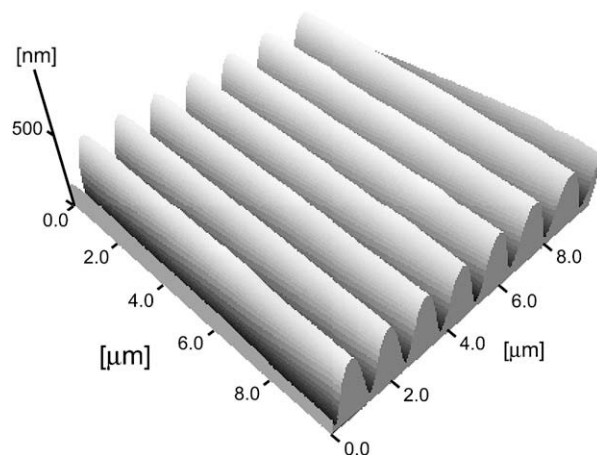


Fig. 5. AFM image of SRG inscribed on CN-BFIAB amorphous film.

4. Conclusion

Novel azobenzene-based photo-responsive amorphous molecular materials, CN-BFIAB and NO₂-BFIAB, were designed and synthesized. They were found to readily form amorphous glasses with relatively high T_gs and to exhibit trans–cis photoisomerizations and reverse cis–trans thermal isomerizations as amorphous films as well as in solution. In addition, relatively large SRGs could be inscribed on both amorphous films of CN-BFIAB and NO₂-BFIAB upon interference exposure to writing laser beams. The modulation depth of the SRG inscribed on the CN-BFIAB amorphous film was found to be larger than that inscribed on the NO₂-BFIAB film, which was attributable to the fact that the photoisomerization for the amorphous film was more suppressed for NO₂-BFIAB than for CN-BFIAB. In addition, SRG-forming property of CN-BFIAB was not significantly reduced relative to that of BFIAB even though the photoisomerization was more suppressed as amorphous film than that for BFIAB. The fact confirmed that increasing T_g of the material enhances the SRG-forming property.

References

- [1] Yu Y, Nakano M, Ikeda T. *Nature* 2003;425:145.
- [2] Kobatake S, Takami S, Muto H, Ishikawa T, Irie M. *Nature* 2007;446:778–81.
- [3] Rochon P, Batalla E, Natansohn A. *Appl Phys Lett* 1995;66:136–8.
- [4] Kim DY, Tripathy SK, Li L, Kumar J. *Appl Phys Lett* 1995;66:1166–8.
- [5] Barret C, Natansohn A, Rochon P. *J Phys Chem* 1996;100:8836–42.
- [6] Kumar J, Li L, Jiang XL, Kim DY, Lee TS, Tripathy SK. *Appl Phys Lett* 1998;72:2096–8.
- [7] Lefin P, Fiorini C, Nunzi J-M. *Pure Appl Opt* 1998;7:71–82.
- [8] Viswanathan NK, Kim DY, Bian S, Williams J, Liu W, Li L, et al. *J Mater Chem* 1999;9:1941–55.
- [9] Fiorini C, Prudhomme N, de Veyrac G, Maurin I, Raimond P, Nunzi J-M. *Synth Met* 2000;115:121–5.
- [10] Natansohn A, Rochon P. *Chem Rev* 2002;102:4139–75.
- [11] Ando H, Tanino T, Nakano H, Shirota Y. *Mater Chem Phys* 2009;113:376–81.
- [12] Ramanujam PS, Holme NCR, Hvilsted S. *Appl Phys Lett* 1996;68:1329–31.
- [13] Pedersen TG, Johansen PM, Holme NCR, Ramanujam PS. *Phys Rev Lett* 1998;80:89–92.
- [14] Stracke A, Wendorff JH. *Adv Mater* 2000;12:282–5.
- [15] Ubukata T, Seki T, Ichimura K. *Adv Mater* 2000;12:1675–8.
- [16] Yamamoto T, Hasegawa M, Kanazawa A, Shiono T, Ikeda T. *J Mater Chem* 2000;10:337–42.
- [17] Gadidei YB, Christiansen PL, Ramanujam PS. *Appl Phys B* 2002;74:139–46.
- [18] Ubukata T, Takahashi K, Yokoyama YJ. *Phys Org Chem* 2007;20:981–4.
- [19] Ubukata T, Yamaguchi S, Yokoyama Y. *Chem Lett* 2007;36:1224–5.
- [20] Ono H, Emoto A, Kawatsuki N, Hasegawa T. *Appl Phys Lett* 2003;82:1359–61.
- [21] Kawatsuki N, Hasegawa T, Ono H, Tamoto T. *Adv Mater* 2003;15:991–4.
- [22] Yang K, Yang S, Kumar J. *Phys Rev B* 2006;73:165204/1–14.
- [23] Nakano H, Takahashi T, Kadota T, Shirota Y. *Adv Mater* 2002;14:1157–60.
- [24] Shirota Y, Utsumi H, Ujike T, Yoshikawa S, Moriwaki K, Nagahama D, et al. *Opt Mater* 2003;21:249–54.

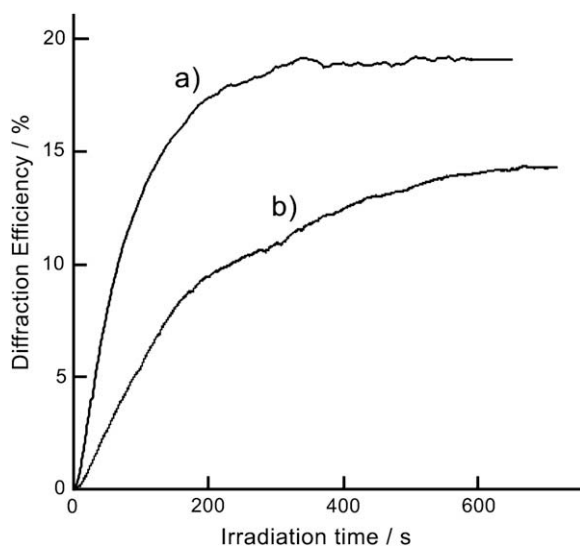


Fig. 4. Growth of diffraction efficiencies for amorphous films upon interference exposure to the writing beams. a) CN-BFIAB. b) NO₂-BFIAB.

- [25] Ueda H, Tanino T, Ando H, Nakano H, Shirota Y. *Chem Lett* 2004;33:1152–3.
- [26] Takahashi T, Tanino T, Ando H, Nakano H, Shirota Y. *Mol Cryst Liq Cryst* 2005;430:9–14.
- [27] Nakano H, Tanino T, Takahashi T, Ando H, Shirota Y. *J Mater Chem* 2008;18:242–6.
- [28] Nakano H, Tanino T, Shirota Y. *Appl Phys Lett* 2005;87:061910/1–3.
- [29] Nakano H. *ChemPhysChem* 2008;9:2174–6.
- [30] Nakano H. *J Phys Chem C* 2008;112:16042–5.
- [31] Fuhrmann T, Tsutsui T. *Chem Mater* 1999;11:2226–32.
- [32] Chun C, Kim M-J, Vak D, Kim DY. *J Mater Chem* 2003;13:2904–9.
- [33] Kim M-J, Seo E-M, Vak D, Kim D- Y. *Chem Mater* 2003;15:4021–7.
- [34] Ishow E, Lebon B, He Y, Wang X, Bouteiller L, Galmiche L, et al. *Chem Mater* 2006;18:1261–7.
- [35] Ishow E, Camacho-Aguilera R, Guerin J, Brosseau A, Nakatani K. *Adv Funct Mater* 2009;19:796–804.
- [36] Nakano H, Takahashi T, Tanino T, Shirota Y. *J Photopolym Sci Tech* 2007;20:87–9.
- [37] Okumoto K, Shirota Y. *Chem Mater* 2003;15:699–707.
- [38] Kageyama H, Itano K, Ishikawa W, Shirota Y. *J Mater Chem* 1996;6:675–6.
- [39] Tanino T, Yoshikawa S, Ujiike T, Nagahama D, Moriwaki K, Takahashi T, et al. *J Mater Chem* 2007;17:4953–63.